

Critical dynamics of superconducting BSCCO films

K. D. Osborn* and D. J. Van Harlingen
Department of Physics and Materials Research Laboratory

Vivek Aji, Nigel Goldenfeld, S. Oh and J. N. Eckstein
Department of Physics
University of Illinois at Urbana-Champaign
1110 West Green Street
Urbana, IL, 61801-3080

(Dated: October 27, 2018)

We report on a systematic investigation of the critical fluctuations in the complex conductivity of epitaxially-grown $\text{Bi}_2\text{Sr}_2\text{CaCu}_2\text{O}_{8+\delta}$ films for $T \lesssim T_c$ using a two-coil inductive technique at zero applied field. We observe the static 3D-XY critical exponent in the superfluid density near T_c . Linear scaling analysis close to the critical temperature yields a dynamic critical exponent of $z \approx 2.0$ for small drive currents, but non-linear effects are seen to be important. At T_c , a non-linear scaling analysis also yields a 3D dynamic exponent of $z = 2.0 \pm 0.1$.

PACS numbers: 74.40.+k, 74.25.Nf, 74.72.Hs, 74.76.Bz

I. INTRODUCTION

Direct observation of the scaling properties of the superconducting transition has at last become feasible due to the discovery of the cuprate superconductors. Microwave measurements in ultrapure single crystal $\text{YBa}_2\text{Cu}_3\text{O}_{7-x}$ (YBCO) have provided strong evidence that for accessible temperature ranges, the effective static universality class is the three dimensional XY model (3D-XY)¹, where the penetration depth displayed scaling over three decades in reduced temperature. Measurements on thin films have yielded varying results: microwave measurements² report $\nu = 1.2$, contactless ac conductivity measurements³ yield $\nu = 1.7$ at frequencies up to 2 GHz and dc conductivity in finite magnetic fields⁴ give $\nu = 0.9 - 1.0$. While none of these agree with the 3D-XY scaling behavior, it is widely believed that the results on pure single crystals are indicative of the intrinsic critical fluctuations of the superconducting transition.

Transport measurements have probed the dynamics of the critical fluctuations, which are characterized by the value of the dynamic critical exponent z describing how the relaxation time τ scales with the correlation length ξ : $\tau \sim \xi^z$. However for YBCO, experiments have not yielded a consistent picture. For example, longitudinal dc-resistivity measurements⁵ yield $z = 1.5 \pm 0.1$ in magnetic fields up to 6T, while microwave conductivity measurements² are consistent with $z = 2.3 - 3.0$. Still larger values for the dynamic exponent ranging from $z = 5.6$ to $z = 8.3$, reminiscent of glassy dynamics, have also been seen in resistivity measurements^{3,4} in thin films. These large values of z strongly suggest that disorder plays a dominant role in these thin films, and this may explain why their observed static critical behavior differs from that of the best single crystals.

Critical fluctuation results on $\text{Bi}_2\text{Sr}_2\text{CaCu}_2\text{O}_{8+\delta}$ (BSCCO) are even more dissimilar, partially due to

highly anisotropic fluctuations. The complex conductivity of underdoped BSCCO films measured at terahertz frequencies was found to agree with a Kosterlitz-Thouless-Berezinskii (KTB) model with diffusive dynamics.^{8,9} In previous work on BSCCO crystals a non-linear transport study found 2D critical behavior with an anomalous dynamic exponent of $z \approx 5.6$ and no crossover to 3D behavior.⁶ The 3D universal phase angle of the complex conductivity deduced from the magnetic susceptibility of BSCCO epitaxial films and crystals has even yielded larger values of z .⁷ Only dc fluctuation conductivity measurements in BSCCO¹⁰ find relaxational dynamics, $z \approx 2.0$, assuming a 3D-XY static exponent, $\nu \approx 2/3$, in agreement with recent theoretical work that predicts that $z \approx 2.0$ in 3D.¹¹ These results indicate the lack of consensus on the true nature of the dynamic fluctuations representative of the superconducting transition, which is the primary motivation of the present investigation. While a large value of the dynamic exponent ($z > 2$) can be understood as disorder effects, only the presence of a previously undetected collective mode coupled to the superfluid density would lead to $z \approx 1.5$ in 3D, just as occurs in superfluid He^{4,12}.

In this paper we provide results on the critical fluctuations in high quality epitaxially-grown BSCCO films. We have measured the ab-plane complex conductivity with a two-coil inductive technique at zero applied magnetic field ($H = 0$), described in Section II. Our measurements, presented in section III, indicate that the critical fluctuations in BSCCO films are consistent with the 3D-XY critical fluctuation model, rather than a KTB transition within the layers. This contrasts with earlier studies using this technique on YBCO, which have reported KTB critical¹³ and mean-field¹⁴ fluctuations. In section IV, we estimate the temperature intervals in which possible crossovers to 2D fluctuations can occur, due either to decoupling of the bilayers or to the thin film behaving as a

2D system with a large c -axis correlation length. We find that our measurements should indeed be well-described by anisotropic 3D-XY critical fluctuations. In section V, we provide a crossover analysis of the approach to the critical point, and examine the approach to a universal phase angle. In particular, we predict the qualitative forms of the variations with temperature and frequency. These are in agreement with our measurements, but contrast earlier results which report very different values of the static and dynamic critical exponents than those reported here. Analysis of the phase angle of the film response using linear response theory in the critical region, which yields a dynamic exponent of $z = 2.0$, is presented in section VI. However, the breakdown of linear response theory becomes important near the transition temperature T_c , so that the analysis is complicated by the need to extract the superfluid density from the measured mutual inductance by an approximate inversion technique. Our analysis shows that the determination of z purely from linear response theory is contaminated by non-linear effects, and at probe currents that are too large the effective value of z inferred can be as low as 1.5. To circumvent this problem, we derive in section VII a non-linear scaling law obeyed by the raw measured mutual inductance at T_c (i.e. without the need for a data inversion) and extract the dynamic exponent directly from the mutual inductance. In agreement with the linear response analysis, we again obtain $z \approx 2.0$. Section VIII summarizes our conclusions.

II. SAMPLES AND EXPERIMENTAL SETUP

We have measured several high quality oxygen-doped BSCCO films, grown by molecular-beam-epitaxy on SrTiO₃ substrates and analyzed *in-situ* by RHEED¹⁶. The BSCCO films are nominally oriented along the c -axis, with unit cell thickness of $d = 15.4$ Å. AFM images of similar BSCCO films reveal an *rms* roughness of 5 Angstroms primarily due to single unit cell step height variation over the surface. The *rms* roughness of the substrates are approximately 1.5 Angstroms.

The inductively-measured T_c from several films of different dopings was fit to the empirical formula $T_c = T_{c,max}(1 - 82.6(p - 0.16))^2$, to determine the hole doping per Cu, p .¹⁵ The two branches of the formula are distinguished by the relative low temperature superfluid density, which is known to increase monotonically through optimal doping ($p=0.16$). Films A, B, and C have $n = 21, 40$ and 60 unit cells respectively and are grown on 10 and 14 mm square substrates. Film A is overdoped at $p \simeq 0.19$, while film B and C are slightly overdoped and underdoped, respectively. We estimate that a doping gradient in the samples introduces a experimental temperature broadening of 0.15 K near T_c .

To obtain the ab-plane complex conductivity, we employ a two-coil inductive technique. The mutual inductance of two coaxial coils is measured with a film placed

in between and normal to the axis of the coils. An ac current is applied through the drive coil; a second coil, attached to a large input impedance lock-in amplifier, measures the fields produced by the drive coil and the screening currents in the film. The coils have 135 turns and an average radius of 1.5 mm. The drive coil is placed 0.35 mm above the film so that at a current of $I = 50\mu\text{A}$ *rms*, the applied ac magnetic field is < 0.1 Gauss normal to the film. Measurements are performed in a He⁴ continuous-flow dewar, which allows the temperature of the film to be controlled without significant heating from the drive coil. The sample temperature is monitored by a Si diode attached to the back side of the substrate.

The complex conductivity $\sigma = \sigma_1 - i\sigma_2$ of each film is calculated from the mutual inductance using the exact analytical expression for an infinite diameter film¹⁷ and a numerical inversion technique similar to that of Fiory *et al.*¹⁸. The method of Turneaure *et al.*¹⁹ is employed to correct for film diameter effects prior to calculating the in-plane complex conductivity. The measured penetration depth $\lambda_{ab} = (\mu_0\omega\sigma_2)^{-1/2}$, is independent of the measurement frequency from $f = 10 - 100$ kHz below the transition temperature, where the dissipation is small ($\sigma_1 \ll \sigma_2$). To analyze the critical fluctuations, we study the complex superfluid density per CuO bilayer, $\rho = i\sigma\omega d\Phi_0^2/(4\pi^2k_B)$, where Φ_0 is the superconducting flux quantum.²⁰ The real part of this quantity, $Re[\rho]$ has units of temperature and sets the energy scale for critical fluctuations. In Fig. 1(a), $Re[\rho]$ obtained at $f = 80$ kHz and $I = 40\mu\text{A}$ is plotted for films A through C. At 5 K, films A, B, and C, have penetration depths of 235, 265, and 285 nm, respectively. Note that film A, which is overdoped, has a smaller low temperature penetration depth than film B and C. All films exhibit a T^2 component to the superfluid density at low temperatures, however the zero-temperature intercept of the films near optimal doping is approximately zero, indicating the crystalline films have very few impurities.

III. STATIC CRITICAL BEHAVIOR

In Figs. 1(a) and 1(b) a power of $\rho = Re[\rho]$ and $2T/\pi$ is shown to locate where we would expect the KTB transition for a noninteracting bilayer, $\rho = 2T/\pi$.²¹ We observe no such drop in the superfluid density at this temperature in our films. The films instead show that coupling among the bilayers induces an anisotropic 3D transition, precluding a KTB transition in the bilayers. At the transition temperature of an isolated bilayer $T = \rho\pi/2$, however, the measured superfluid density has been renormalized from the mean field value by quasi-2D fluctuations.

The mean field behavior, expected at low temperatures, crosses over to the 3D-XY behavior as the critical temperature is approached from below. In layered systems, the 3D-XY behavior is exhibited once the c -axis correlation length exceeds the interlayer spacing, d ; i.e. when $\rho(T) = c_s T_c$, where $c_s \approx 0.5$ and $\rho = Re[\rho]$.¹

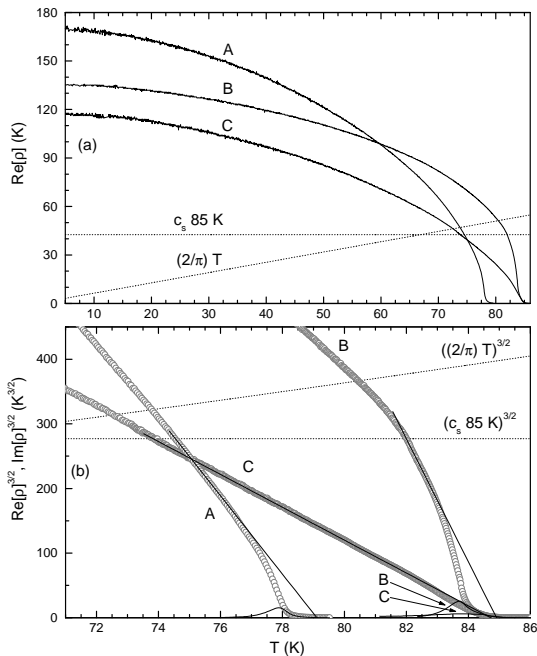


FIG. 1: $Re[\rho]$ (panel a) and $Re[\rho]^{3/2}$ (panel b), as a function of temperature for films A through C. $\rho = (c_s 85\text{K})$ is the predicted crossover to 3D-XY critical behavior and $\rho = (2/\pi)T$ is the KTB critical superfluid density for an isolated bilayer.

In Fig. 1(b), the data from Fig. 1(a) are plotted as $Re[\rho]^{3/2}$ near the critical regime. Also shown in Figs. 1(a) and 1(b) is the corresponding power of $c_s T_c$ to locate the onset of 3D-XY behavior. The static 3D-XY model gives $\rho \sim \xi^{-1} \sim |T - T_c|^\nu$, where $\nu \approx 2/3$. We observe that $Re[\rho]^{3/2}$ varies linearly in temperature for $\rho(T) \lesssim c_s T_c$ indicating a 3D-XY, rather than mean-field ($\rho \sim |T - T_c|$), behavior. At our measurement current ($40\mu\text{A}$), we observed an absence of frequency dependence below the dissipation peak over the temperature range of the fit. In film C, the linear regime extends as far as 7 K below 82 K. The linear fits extrapolate to $T_c = 79.1\text{ K}$, 84.9 K and 84.7 K for films A, B and C respectively.

Although our static scaling analysis is carried out at temperatures and at a drive current for which there is no discernible frequency dependence, at higher temperatures we observe variations with both drive current and frequency. This is apparent in Fig. 2, for which larger currents are used on film B with 40 layers. Film C, with 60 layers, exhibited a weaker dependence over the same frequencies and currents. Since the superfluid density depends on frequency and current at higher temperatures, the superfluid density scales as $\rho \sim \xi^{2-D} f(\omega\xi^z, E\xi^{1+z})$, where E is the amplitude of the electric field. Only in the critical regime where the data are independent of both frequency and electric field can one expect to see the linear response scaling behavior and extract the exponent

ν . At higher temperatures where we observe non-linear behavior as well as frequency dependence, the data are still consistent with the 3D-XY fluctuations, and we can extract z . In section VI we analyze the phase angle in

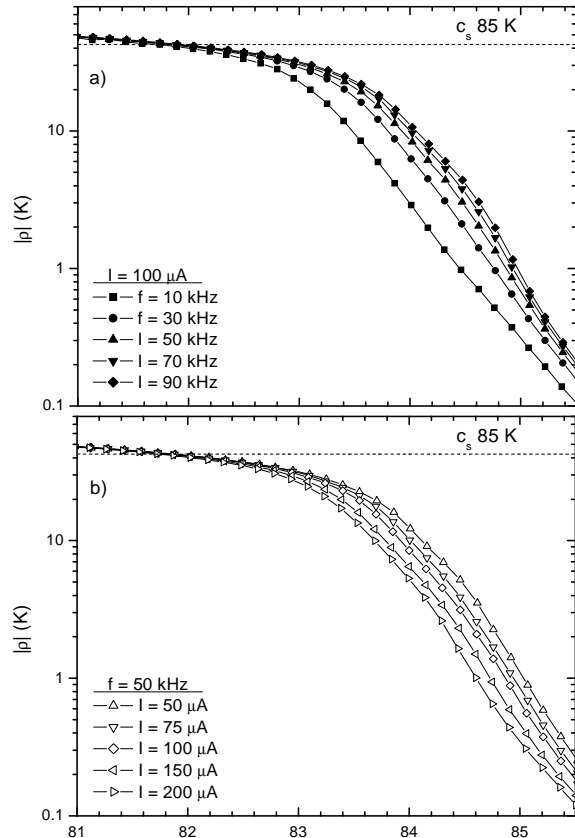


FIG. 2: $|\rho|$ in film B taken at a series of frequencies (panel a) and drive currents (panel b).

IV. DIMENSIONALITY OF THE STATIC FLUCTUATIONS

When the superfluid density is a fraction of the 3D crossover ($\rho(T) < (1/2)c_s T_c$), we observe a drop in the superfluid density from the static scaling value. Although this could be interpreted as a crossover to 2D behavior, we do not believe this to be the case in our films since the drop is observed to be current as well as frequency dependent (see Fig. 2). Notice that the superfluid density does drop more rapidly than expected from the 3D-XY model as the frequency is decreased for a given drive current, but does so more slowly as the current is decreased at fixed frequency. While the former might lead one to conclude that the anisotropic 3D-XY behavior is no longer valid in the static limit, the latter would imply the opposite. More accurate measurements are needed at low

frequency and currents to establish unambiguously the true nature of the static limit. Nevertheless the trend with decreasing current, coupled with the phase angle dependence discussed in the next section, is consistent with 3D-XY behavior. Another putative crossover to 2D behavior is expected when ξ_c becomes as large as the film thickness, h . The 3D-XY scaling implies that this occurs at a temperature, T^* , which is 0.05 K, 0.01 K and 0.02 K below the transition temperature for films A, B and C respectively. This implies that the region of pure 2D fluctuations is too small to be resolved in our data and therefore we expect 3D fluctuations to dominate.

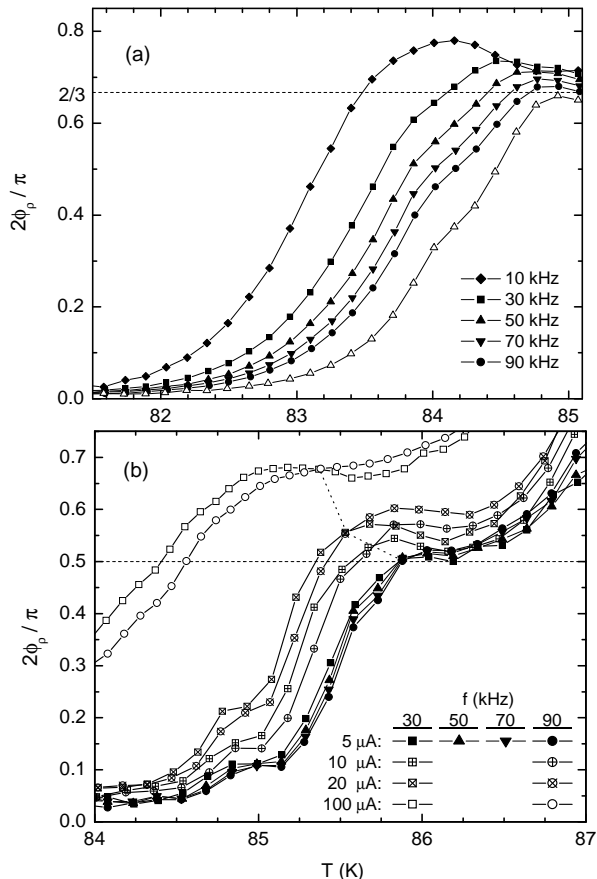


FIG. 3: Normalized phase angle, $2\phi_\rho/\pi$, of the superfluid density extracted from linear response theory. Panel a: $2\phi_\rho/\pi$ in film B taken at $I = 100\mu\text{A}$ (filled symbols) at a series of frequencies and $I = 50\mu\text{A}$ for $f = 50\text{kHz}$ (unfilled triangles). Panel b: $2\phi_\rho/\pi$ in film C for a given table of frequencies and drive currents.

V. CROSSOVER PHENOMENA IN THE LINEAR PHASE ANGLE NEAR T_c

Since the experiments are performed at finite frequency, it is important to consider whether or not the correct asymptotic behavior is being probed and what

conclusions can be drawn from the observed behavior. We begin with the superfluid density, within linear response, written as

$$\rho = (t^{-\nu})^{2-D} f_1(\omega t^{-\nu z}) \quad (1)$$

where $t = |T - T_c|/T_c$ and f_1 is a scaling function. In the limit of $t \rightarrow 0$ ($T \rightarrow T_c$), the t -dependence must cancel out of the expression for ρ , which implies that the asymptotic behavior of the scaling function $f_1(x) \sim x^\theta$ as $x \rightarrow \infty$ where $\theta = (2 - D)/z$. For $t \neq 0$, we can write

$$\rho = (i\omega)^{(D-2)/z} f_2(t\omega^{-1/\nu z}) \quad (2)$$

where the scaling function $f_2(y) = \text{const}$ as $y \rightarrow 0$. We now ask what behavior we should observe as $\omega \rightarrow 0$ for $t \neq 0$. For $\omega \rightarrow 0$ at $t = 0$, we should see the critical point behavior. For $t/\omega^{1/\nu z} \ll 1$ we are probing the $y \sim 0$ regime of the scaling function $f_2(y)$ and expect to see asymptotic scaling behavior. If $t/\omega^{1/\nu z} \gg 1$ we are probing the $y \rightarrow \infty$ regime of the argument of f_2 and do not expect to see the scaling behavior. Thus at a finite t_0 , for $\omega \gg t_0^{4/3}$ we would observe critical behavior while for $\omega \ll t_0^{4/3}$ we would not. We have used the critical exponents $\nu = 2/3$ and $z = 2$ for specificity, but the argument does not rely on these precise values. Note that, as is generally the case with crossover, the behavior of the superfluid density away from the critical point at finite frequencies is not universal except in the large frequency limit - a result that is sometimes found to be surprising, but which follows from a generic crossover analysis of relevant variables.²² This predicted low frequency behavior is consistent with our data where we observe the critical phase angle in Fig. 3(b) and yet we do not observe scaling below T_c . More importantly, this is also consistent with the non-linear scaling observed at T_c in Section VII. Away from T_c an asymptotic scaling regime is demonstrated in the microwave measurements of Booth *et al.*²

VI. DYNAMIC CRITICAL BEHAVIOR AND THE BREAKDOWN OF LINEAR RESPONSE THEORY

Next we study the phase of ρ , ϕ_ρ , close to the transition temperature. The frequency dependence of $2\phi_\rho/\pi$ for film B measured at $I = 100\mu\text{A}$ is shown in Fig. 3(a). Within linear response theory, the phase angle is independent of frequency at the critical temperature and is given by $\phi_\rho(T_c) = \pi/(2z)$ in three dimensions, where z is the dynamic critical exponent.²³ In Fig. 3(a) we notice that the curves for different frequencies seem to approach a phase angle consistent with a dynamic exponent of $z \approx 1.5$ and $T_c = 84.9$ K. When repeated at a smaller value of the current, $I = 50\mu\text{A}$, $\phi_\rho(T_c)$ is smaller, as shown. Since the constant phase angle is a result from

linear response theory, the estimate of the dynamic exponent from the data is expected to be more accurate at smaller currents.

This is indeed seen in the current dependence of the phase angle at different frequencies for film C. In Fig. 3(b), $2\phi_\rho/\pi$ is shown for a set of frequencies and currents. As the current is lowered, the frequency independent phase angle shifts to lower values. At $20\mu\text{A}$, $10\mu\text{A}$ and $5\mu\text{A}$, this phase angle is $0.57\pi/2$, $0.54\pi/2$ and $0.51\pi/2$ respectively. This suggests that $z \simeq 2.0$ in film C and the result of $z \approx 1.5$ from film B is an artifact of the large current used in the measurement. With this analysis, the thickest film (C) exhibits the best estimate of the critical phase angle, the film with intermediate thickness (B) provides evidence for similar behavior, but the thinnest film did not show a critical phase angle. Due to the crossover phenomena discussed in the previous section, the behavior of the phase angle away from T_c is not universal at low frequencies, but we can still infer the dynamic critical exponent from the critical phase angle at T_c which is indeed universal.

Both the phase angle and the superfluid density are found to be dependent on the drive current near T_c . In the limit of smaller currents, the frequency independent critical phase angle does indeed yield a dynamic exponent of $z \approx 2.0$. This is a result consistent with the presence of 3D fluctuations. This is also consistent with the behavior of the superfluid density with decreasing current at fixed frequency, where it is seen to approach the asymptotic static scaling law. Furthermore, the smooth evolution of the phase angle suggests that the crossover to the 2D regime near T^* is not resolved in our experiment. Nevertheless, considering that nonlinear scaling and dimensional crossover is expected close to T_c , we now proceed to analyze the nonlinear response to get a more accurate determination of the dynamic exponent.

VII. NONLINEAR SCALING AT THE SUPERCONDUCTING TRANSITION

The field equation governing the vector potential, \vec{A} , is

$$\nabla^2 \vec{A}/\mu_0 = -\vec{J}_d - h\delta(z)\sigma\vec{E} \quad (3)$$

where \vec{J}_d is the current density in the drive coil, σ is the conductivity of the superconducting film, and \vec{E} is the electric field. For the geometry of the setup,

$$\vec{J}_d = I_d\delta(r - r_c)\delta(z - z_c)\hat{\phi} \quad (4)$$

in cylindrical coordinates, where I_d is the drive current, r_c is the radius of the drive coil and z_c is the distance from the film to the drive coil.¹⁷ For an anisotropic system, in the critical regime, the superfluid density, ρ , scales as,

$$\rho \sim i\omega\sigma \sim \xi_{ab}^{3-D}\xi_c^{-1}f(i\omega\xi_{ab}^z, E\xi_{ab}^{1+z}) \quad (5)$$

where ξ_{ab} and ξ_c are the correlation lengths parallel and perpendicular to the CuO bilayers, and f is a scaling function. We can rewrite the field equation as

$$\begin{aligned} \nabla^2 A = & -\mu_0 I_d \delta(r - r_c) \delta(z - z_c) \\ & - h \xi_{ab}^{3-D} \xi_c^{-1} f(\omega \xi_{ab}^z, A \xi_{ab}) A \delta(z) \end{aligned} \quad (6)$$

where we have used the scaling form for the complex conductivity. Since the scaling function is written in terms of dimensionless variables we can non dimensionalize the equation by recasting it in terms of $A\xi_{ab}$, $\omega\xi_{ab}^z$, r/h and $I_d\xi_{ab}$. The solution then takes the form,

$$Ai\omega\xi_{ab}^{1+z} = G(i\omega\xi_{ab}^z, i\omega\xi_{ab}^{1+z}I_d, h^2\xi_{ab}^{3-D}\xi_c^{-1}\Lambda^{-1}, r/h) \quad (7)$$

where G is a function that can be determined by solving the full non-linear field equation and Λ is the thermal length given by $\Phi_0^2/(4\pi\mu_0 k_B T)$. So far all we have done is to use the scaling form for the superfluid density and looked for a generic solution of a differential equation by identifying all the non-dimensional variables. For a given geometry of the experiment the right hand side of Eq. 7 is a function of three variables. One can further simplify the expression if we realize that there exists a regime $|T - T_c| < T^*$ where we are governed by the limit where $\xi_c = h$. This allows us to eliminate one of the three terms as follows. Close to T_c , using the 3D-XY behavior of the correlation length and the definition of T^* , we can rewrite $h^2\xi_{ab}^{3-D}/\xi_c$ as,

$$h^2\xi_{ab}^{3-D}/\xi_c = h|1 + (T - T^*)/(T^* - T_c)|^\nu. \quad (8)$$

For a temperature range $|T - T^*| \ll |T^* - T_c|$, $h^2/\xi_c \approx h$. Thus, for temperatures within $0.05K$, $0.02K$, and $0.01K$ of T^* for films a, b, and c respectively, this approximation is valid, and the field in Eq. 7 is a function of only two variables for a given geometry. Thus one can now perform the standard data collapse at T_c of the measured mutual inductance to obtain the dynamic exponent. In this regime we can eliminate ξ_{ab} from Eq.7 so that

$$A = \omega^{1/z} \tilde{G}(I_d \omega^{-1/z}, h \Lambda^{-1}, r/h). \quad (9)$$

The mutual inductance, M , is related to the vector potential at the pick up coil and scales as

$$M \sim A\omega^{-1/z} \sim \tilde{G}(I_d i\omega^{-1/z}). \quad (10)$$

Within the resolution of our data, any data collapse observed is a 3D phenomena starting to crossover to the asymptotic 2D scaling. The reason for this is that the solution (Eq. 7) depends on a number of variables, but sufficiently close to T_c there exists a regime wherein the mutual inductance is only a function of one scaling variable. If we do not observe any data collapse we would conclude that we are never in the regime where the approximation $h^2/\xi_c \approx h$ is valid. It is indeed true that the elimination of the dependence of ξ_{ab} in Eq. 7 is possible only at T_c and need not hold in the entire regime

where the crossover occurs. It is tempting to interpret the experimental results in terms of a 2D system. Our data on the other hand are unable to resolve the crossover regime, and yet do exhibit data collapse (see Fig 4). This suggests that the temperature at which we observe data collapse lies in the crossover regime, but is not necessarily the true T_c . From our analysis we conclude that the T_c is within 0.02 K of the temperature at which we observe data collapse for film B and C. We now look for data collapse of our data measured by varying frequency, current and temperature. Notice that the value of the exponent ν is required only to establish the regime of validity of the approximation and is not necessary to extract the dynamic exponent from data collapse at T_c .

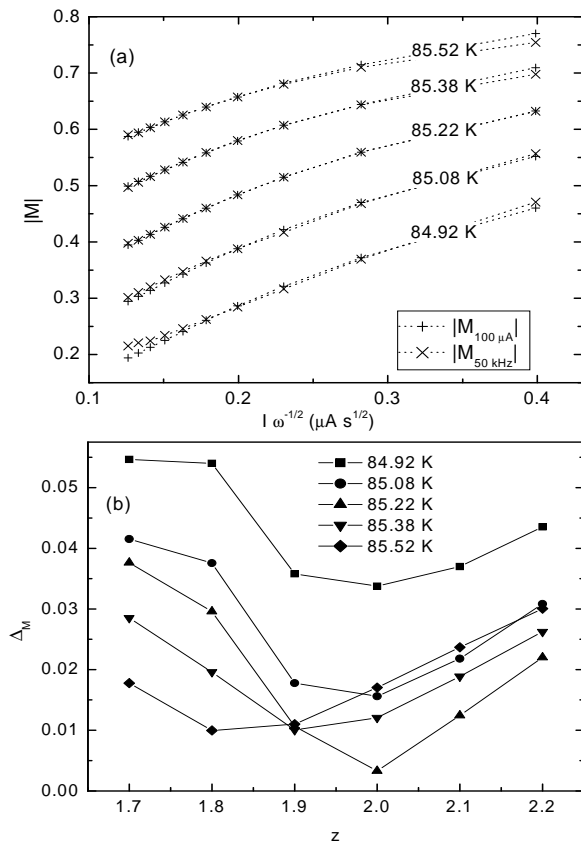


FIG. 4: Panel (a): $|M|$ measured at $I = 100\mu\text{A}$ and $f = 50$ kHz versus the scaling variable $I\omega^{-1/2}$. Panel (b): Scaling error at different temperatures versus z .

For the scaling analysis at T_c , the mutual inductance at fixed frequency, M_f , was compared to the mutual inductance at fixed current, M_I . For convenience, $|M(T)|$ is normalized to unity above the T_c . Values of M_f (M_I), were measured at $12.5 \mu\text{A}$ (10 kHz) intervals for a set of fixed temperatures. Then values of $|M_f|$ were compared with values of $|M_I|$ taken at the same temperature

by fitting the raw data of $|M_f|$ to a polynomial and selecting points with the values of $I\omega^{-1/z}$ equivalent to those of $|M_I|$. In Fig. 4(a) $|M_f|$ and $|M_I|$ for film B are plotted versus $I\omega^{-1/2}$ for a series of temperatures. The best data collapse of the curves appear at $z = 2.0$ and $T = 85.22$ K. The error in the scaling, Δ_M , is shown in Fig. 4(b) for different temperatures and values of z . This is obtained from $\Delta_M^2 = \sum (|M_f| - |M_I|)^2$, where the sum runs over the 10 values of $I\omega^{-1/z}$ measured for $|M_I|$. The lowest error value indicates $z = 2.0 \pm 0.1$ and $T = 85.2 \pm 0.1$ K. A similar analysis for the film C yields $z = 1.8 \pm 0.2$ and $T = 85.9 \pm 0.2$ K, which is also consistent with $z = 2.0 \pm 0.1$. The transition temperature of film B is $T_c = 85.2 \pm 0.1$ K, while for film C it is $T_c = 85.9 \pm 0.2$ K. These values of T_c are close to those obtained with the phase angle measurements.

In Fig. 4(b), the evolution of the error for a fixed trial z also suggests that the dynamic exponent observed is indeed due to 3D fluctuations. Notice that as the temperature is increased for $z = 2.0$, the error decreases, approaching the best fit (i.e. data collapse), and then increases again. Within the resolution of the data, we never observe any change to the 2D regime. In other words, the approximation that allowed us to look for the data collapse is indeed supported by the behavior of the mutual inductance.

VIII. CONCLUSIONS

The superfluid density in BSCCO films with different thicknesses has been measured and shown to be consistent with the predictions of the 3D-XY model. The dynamic scaling exponent has been obtained by performing both a linear and non-linear scaling analysis. While the linear scaling analysis did yield a 3D dynamic exponent of $z \approx 2.0$, non-linear effects needed to be studied to get an accurate determination. This is evident from the current dependence of the critical phase angle of the superfluid density. A 3D non-linear scaling analysis also yields a dynamic exponent of $z = 2.0 \pm 0.1$.

Acknowledgments

We thank H. Westfahl and D. Sheehy for many helpful discussions. This work was supported by the U. S. Department of Energy, Division of Materials Sciences, grant DEFG02-91ER45439 through the Frederick Seitz Materials Research Laboratory at the University of Illinois at Urbana-Champaign, and by the National Science Foundation under grant number NSF-DMR-99-70690.

-
- * Present address: National Institute of Standards and Technology, Boulder, CO, 80305
- ¹ S. Kamal, D.A. Bonn, N. Goldenfeld, P.J. Hirshfeld, R. Liang, and W.N. Hardy, Phys. Rev. Lett. **73**, 1845 (1994).
 - S. Kamal, R. Liang, A. Hosseini, D.A. Bonn, and W.N. Hardy, Phys. Rev. B **58**, R 8933 (1998).
 - ² J.C. Booth, D.H. Wu, S.B. Qadri, E.F. Skelton, M.S. Osofsky, A. Pique, and S.M. Anlage, Phys. Rev. Lett. **77**, 4438 (1996).
 - ³ G. Nakielsky, D. Gorlitz, Chr. Stodte, M. Welters, A. Kramer and J. Koetzler, Phys. Rev B **55** 6077 (1997).
 - ⁴ J.M. Roberts, B. Brown, B.A. Hermann and J. Tate, Phys. Rev. B **49**, 6890 (1994).
 - ⁵ J.T. Kim, N. Goldenfeld, J. Giapintzakis and D.M. Ginsberg, Phys. Rev. B **56**, 118 (1997).
 - ⁶ S.M. Ammirata, M. Friesen, S.W. Pierson, L.A. Gorham, J.C. Hunnicutt, M.L. Trawick and C.D. Keener, Physica C **313**, 225 (1999). S.W. Pierson, M. Friesen, S.M. Ammirata, J.C. Hunnicutt and L.A. Gorham, Phys. Rev. B. **60**, 1309 (1999).
 - ⁷ J. Kotzler and M. Kaufmann, Phys. Rev. B **56**, 13734 (1997).
 - ⁸ J. Corson, R. Mallozzi, J. Orenstein, J.N. Eckstein, and I. Bozovic, Nature **398**, 221 (1999).
 - ⁹ P. Minnhagen, Rev. Mod. Phys. **59**, 1001 (1987).
 - ¹⁰ S.H. Han, Y. Eltsev and O. Rapp, Jour. Low. Temp. Phys. **117** 1259 (1999). S.H. Han, Y. Eltsev and O. Rapp, Phys. Rev. B. **61**, 11776 (2000).
 - ¹¹ V. Aji and N.D. Goldenfeld, Phys. Rev. Lett **87**, 197003 (2001).
 - ¹² P.C. Hohenberg and B.I. Halperin, Rev. Mod. Phys. **49**, 435 (1977).
 - ¹³ A.T. Fiory, A.F. Hebard, P.M. Mankiewich and R.E. Howard, Phys. Rev. Lett. **61** 1419 (1988).
 - ¹⁴ Z.H. Lin, G.C. Spalding, A.M. Goldman, B.F. Bayman, and O.T. Valls, Europhys. Lett. **32**, 573 (1995). K.M. Paget, B.R. Boyce, and T.R. Lemberger, Phys. Rev. B **59**, 6545 (1999).
 - ¹⁵ M.R. Presland, J.L. Tallon, R.G. Buckley, R.S. Liu, and N.E. Flower, Physica C **176**, 95 (1991).
 - ¹⁶ J.N. Eckstein, I. Bozovic, K.E. von Dessionneck, D.G. Schlom, J.S. Harris Jr., and S. M. Baumann Appl. Phys. Lett. **57**, 931 (1990).
 - ¹⁷ J.R. Clem and M.W. Coffey, Phys. Rev. B **46**, 14662 (1992).
 - ¹⁸ A.T. Fiory, A.F. Hebard, P.M. Mankiewich, and R.E. Howard, Appl. Phys. Lett. **52**, 2165 (1988).
 - ¹⁹ S.J. Turneaure, E.R. Ulm, and T.R. Lemberger, J. Appl. Phys. **79**, 4221 (1996). S.J. Turneaure, A.A. Pesetski, T.R. Lemberger, Jour. Appl. Phys. **83**, 4334 (1998).
 - ²⁰ D.S. Fisher, M.P.A. Fisher and D.A. Huse, Phys. Rev. B **43** 130 (1990).
 - ²¹ M.R. Beasley, J.E. Mooij and T.P. Orlando, Phys. Rev Lett **42**, 1165 (1979).
 - ²² N. Goldenfeld, *Lectures on Phase Transitions and the Renormalization Group* (Addison-Wesley, Reading, Mass., 1992), p. 271.
 - ²³ A.T. Dorsey, Phys. Rev. B **43**, 7575 (1991).